Cosmic-ray double-core γ-family events at ultrahigh energies

Z. Cao
Institute of Theoretical Science and Department of Physics, University of Oregon, Eugene, Oregon 97403

L. K. Ding and Q. Q. Zhu
Cosmic Ray Laboratory, Institute of High Energy Physics, Academia Sinica, Beijing 100039, People's Republic of China

Y. D. He
Department of Physics and Space Science Laboratory, University of California, Berkeley, California 94720 and Nuclear Science Division and Institute for Nuclear and Particle Astrophysics, Lawrence Berkeley National Laboratory, Berkeley, California 94720

(Received 26 June 1996)

We present a detailed account of our analysis on ultrahigh-energy cosmic-ray double-core γ-family events observed in emulsion chambers at mountain levels. Extending the leading-order perturbative QCD jet calculations for hadron-hadron collisions to hadron-nucleus collisions by including nuclear effects, we performed a Monte Carlo simulation of cosmic-ray particle interaction and propagation in the atmosphere. We find a significant excess of event rates at large transverse momenta with respect to our prediction based on perturbative QCD. The excess cannot be accounted for by a compositeness model of quarks with a characteristic energy scale lower limit $\Lambda_c > 1.4$ TeV or a possible value of $\Lambda_c \simeq 1.6$ TeV from the CDF at the Fermilab Tevatron. We discuss possible onset of new physics indicated by the large discrepancy at $E_{\rm lab} \sim 10^4 - 10^5$ TeV, an energy region beyond the reach of existing colliders but within the range of future hadron colliders such as the proposed Large Hadron Collider at CERN. [S0556-2821(97)06823-9]

PACS number(s): 13.85.Tp, 12.38.Qk, 12.60.Rc, 96.40.De

I. INTRODUCTION

Several emulsion chamber experiments installed on mountain tops at high altitudes have taken data for more than a decade. The major goals of these experiments are to search for new high-energy phenomena and to explore the mechanism of nuclear collisions in an energy regime not yet accessible to current accelerators or colliders. A typical atmospheric cosmic-ray event registered in such experiments is the so-called γ family. A γ family consists of a bundle of high-energy particles incident on the chamber in almost the same direction. Each observed particle in a family has a visible energy above the threshold of the detector (usually $\sim 2-4$ TeV). A γ-family event contains the electromagnetic component near the core of an atmospheric cascade resulting from cosmic-ray interactions with the atmospheric targets. Efforts have been made by several groups of authors [1–3] to extract useful information from the γ-family phenomenon about characteristics of multiparticle production in hadron-hadron interactions as well as information about the spectrum and composition of primary cosmic rays at lab energy of $10^{15}-10^{17}$ eV.

Several classes of exotic events with unusual features have been reported, indicating new physics of the strong interaction at energies at least one order of magnitude higher than that of current accelerators. Examples are Centauro (and mini-Centauro) events, coplanar (or cluster alignment) events, concentric (or ringlike) events, and double-core (or binocular) events. Of a particular interest one is the double-core events in which most particles or energy flows in a family are spatially distributed in two clusters. Two experimental groups have consistently found that $\sim 7\%$ of γ families exhibit such a behavior. It has been pointed out that the two cluster configuration of cosmic-ray events has a connection to high transverse momentum (p_T) jet production [4]. Since then several detailed analyses have shown that the QCD-jet production is indeed the physics that is responsible for the double-core structure. For coplanar structure, explanations were suggested based on QCD-jet production by Halzen and Morris [5] and based on single diffractive dissociation by He *et al.* [6].

In a recent Letter [7], we briefly reported the major results of our studies of double-core phenomena. We emphasized the significant excess of event rates at large transverse momenta with respect to the prediction of perturbative quantum chromodynamics (PQCD). In this paper, we present a detailed account of our systematic analysis of cosmic-ray double-core events with additional new calculations of general properties of γ-family events. In Sec. II, we discuss some general features of cosmic-ray study of the strong interaction, focusing on issues that we want to address in this paper. Section III briefly reviews the experimental aspects of γ-family observations at mountain levels. In particular, we discuss the selection criteria of double-core events and the data set we used in this analysis. Section IV is devoted to a presentation of the interaction models used in our Monte Carlo simulations. It includes discussions of the PQCD calculation of high-p_T physics and a conventional model of low-p_T physics of hadron-hadron interactions, our treatment of nuclear effects in hadron-nucleus interactions, and an effective theory of the compositeness of quarks. In Sec. V, we outline our Monte Carlo simulation of γ-family phenomena, including the interaction and propagation of cosmic-ray particles in the atmosphere, and the response of detectors. In

Sec. VI, we compare our simulation results with the data including the general properties of γ-family events and the special features of double-core events. After discussing possible onset of new physics indicated by double-core events, we summarize our conclusions and present additional comments in Sec. VII.

II. STUDY OF NEW PHYSICS FROM γ-FAMILY PHENOMENA

To study the underlying physics of exotic phenomena in ultrahigh energy cosmic-ray events, it is very important to consider the background and fluctuations carefully. This becomes even more critical for γ-family phenomena as can be seen in the following.

Particles recorded in a family event are products of multiple collisions and cascades of primary cosmic-ray particles in the atmosphere above the observational level. Multiple particle production plays an essential role in the formation of γ families. The cascade feature as well as the bias in the observation leads to the indispensability of the Monte Carlo simulation of the interaction, decay, and propagation of ultrahigh-energy cosmic-ray particles in the atmosphere. The Monte Carlo method appears to be the best way so far to compare the model predictions with the data under the same biased condition. Moreover, a variety of uncertainties involved in the multiparticle production model requires a Monte Carlo generator to simulate the interaction process.

We have pointed out before [6,8] that one of the features of the study of hadronic interactions by γ families is the biased detection. There are many reasons for biased recording. First of all, the particles observed in emulsion chambers are the products of multiple successive interactions and cascades in the atmosphere rather than one single interaction. Our simulation showed that for γ-family events with visible energies $\Sigma E_\gamma = 100-1000$ TeV they experience $\sim 5-6$ times as many collisions on average during their propagation in the atmosphere. The thick atmosphere target above the observation level ($500-600$ g cm^{-2}) corresponds to $\sim 9-12$ mean free paths for hadron-nucleus interactions at these energies. Therefore, events having fewer interactions during their propagation, lower multiplicities in each reaction, and slower energy attenuation in the atmosphere would have larger recording probability in emulsion chambers. Secondly, the energy threshold is quite high (usually $\sim 2-4$ TeV). As a consequence of this high threshold, the Feynman variable x_F spectrum of observed particles is much flatter than that of all particles produced in one interaction, showing that most of the particles with small x_F are absorbed during the atmospheric propagation and only a small fraction of the particles in the fragmentation region is observed. More precisely, if we define the region with x_F larger than 0.05 as the fragmentation region, we find that more than 95% particles recorded in a γ-family event are in the fragmentation region and less than 5% are in the central region due to fluctuations in every interaction. Therefore, it is very important to know the energy dependence of the behavior in the fragmentation, because the way in which the energy is subdivided into individual hadronic interactions determines how far showers penetrate into the atmosphere. Finally, our simulation shows that most of the particles ($\geqslant 90\%$) recorded in emulsion chambers have pseudorapidity in center-mass-system $\eta_{\text{c.m.s.}} > 4$, i.e., the extremely forward region of small angles. Furthermore, more than half of the particles recorded have $\eta_{\text{c.m.s.}} > 6$, a difficult region to observe in a collider experiment. This leads to the claim that cosmic-ray experiments and collider experiments are complementary to each other in terms of sensitive phase space.

Therefore, it is clear that each γ-family event recorded in emulsion chambers does not correspond to a single interaction. Nevertheless, it has been shown that observables attainable in these experiments are still sensitive to characteristics of cosmic-ray interactions with atmospheric target nucleus. For example, the intensity of γ families at a given observational level is determined by the inelastic cross section, multiplicity, inelasticity for hadronic interactions, and their energy dependences. The lateral spread of γ rays in a family is related mainly to the mean value of p_T in the primary interactions as well as the primary composition.

It is of particular interest to note that the observable χ_{12} in double-core events appears to be an indicator of the transverse momentum in the interaction of cosmic-ray particles with the atmospheric target. Experimentally, χ_{12} is defined as $R_{12}\sqrt{E_1 E_2}$ where E_1 and E_2 are energies of the two clusters and R_{12} is the distance between the two clusters. The existence of events with unusually large χ_{12} implies high p_T particle production in the fragmentation region. In order to explain the double-core family data obtained from Kanbala and Chacaltaya experiments, we use a conventional model of hadronic interactions as a starting point. We built a hadron-hadron inelastic interaction model in two sectors: *single-diffraction* (SD) dissociation and *non-single-diffraction* (NSD) dissociation. We developed a hard+soft two-component model for the NSD interaction. The dynamics of high-p_T jet production in the hard component which is the essential mechanism responsible for cluster phenomena is described by perturbative QCD. The soft process is phenomenologically described by a modified version of the geometric model proposed originally by Chou and Yang [9]. The failure of this conventional model to explain the large χ_{12} events would indicate the possible onset of new physics.

In the QCD parton-parton scattering, we include the direct production of high-p_T mesons due to a higher twist correction of QCD [10]. Because the production cross section is proportional to $\alpha_s^3 f_\pi^2$, the enhancement in the production of high-p_T particles due to this process is found to be $\leqslant 10^{-4}$ compared to the leading order contribution. We therefore conclude that higher twist correction could not be important for the excess of event rates at high p_T. Higher order corrections in perturbative QCD calculations are not included in our present calculations. From the recent calculation of Giele *et al.* [11], it appears that the next-to-leading order corrections become important at Fermilab energies and make significant contribution in the region of high transverse momenta and large rapidities. We shall comment on the effect of the next-to-leading order corrections on the rate of double-core events in Sec. VII.

We extend this two component model to hadron-nucleus collisions by taking into account nuclear target effects. The expectation is that the nuclear effects will have important contribution to the enhancement of high-p_T particle production by multiscattering. The most significant one is the so-

called Cronin effect. Experiments [12] have shown that the cross section for high-p_T process in pA interactions is enhanced compared to that in pp interactions by a factor of $A^{\alpha(p_T)}$. The exponent index $\alpha(p_T)$ has been found to be greater than unity in the high-p_T region. For this reason, the effect is also called abnormal nuclear enhencement (ANE) of high-p_T production. This type of enhancement has been found at both the jet level and particle production level. We include this nuclear effect in our simulation model for both hard and soft components.

We also consider new physics that might be responsible for high-p_T particle production at higher energies. In particular, we introduce the effective theory of quark compositeness as a new physics mechanism. The even harder scattering between preons produces even higher-p_T particles.

III. DOUBLE-CORE γ-FAMILY EVENTS AND DATA SETS

Four large-scale emulsion chamber experiments have been carried out for more than one decade. They are experiments on Mt. Kanbala (5500 m) [2], Mt. Chacaltaya (5200 m) [1], Mt. Pamir (4300 m), and Mt. Fuji (3750 m) [2]. The total accumulated collecting power has been up to ~ 5000 m^2 yr for the four experiments. In each experiment, emulsion chamber is composed of multilayers of photosensitive films interleaved with plates of absorbers (lead or iron). Each photosensitive layer contains highly sensitive x-ray films or the combination of x-ray films with nuclear emulsion plate (the use of emulsion is for calibration). The total thickness of a chamber is about 14 radiation lengths or more, so that each chamber is suitable for detecting the electromagnetic component (γ rays and electrons) in cosmic-ray showers. An electron or a photon (electromagnetic component, abbreviated as γ ray hereafter) incident on the chamber initiates an electromagnetic cascade inside the chamber. The development of the cascade is recorded as a series of black spots on the x-ray films ranging over several layers in the chamber. With a calibration using emulsion plates, the optical density of showers on every layer of x-ray film represents the shower longitudinal profile. If the γ ray has an initial energy higher than 4 TeV, measurements of its longitudinal development permit the determination of its energy to within 20% accuracy based on the cascade theory. For a γ ray, the detection efficiency is nearly 100% as long as its energy is higher than 4 TeV. For hadrons, only those interacted inside the chamber and induced electromagnetic showers can be detected. Therefore, the detection efficiency for the hadronic component is much lower than 100% and the detection threshold is higher than that for γ rays, depending on the structure of the chamber. Cascade showers in each family are statistically identified as two categories: γ rays and hadrons. In principle, a chamber is equivalent to a shower calorimeter. The lack of timing information in this passive calorimeter does not count as a disadvantage here because of the extremely low event rates (~ 0.3 m^{-2} yr^{-1}). In Fuji and Kanbala experiments, simple structure chambers are used. In these experiments, γ rays are identified as showers with starting depth less than 6 radiation lengths, with no accompanying successive interactions in the chamber, and others are identified as hadrons. In the other two experiments, in order to detect hadrons more efficiently two chambers separated by light target material (carbon blocks) are used. A sophisticated procedure is adopted to distinguish hadrons from γ rays. The detail of experimental issues can be found in Refs. [1,2], and references therein.

A family event is experimentally identified by requiring that showers of family members are parallel to each other. The direction of a family is determined by zenith angle and azimuthal angle to within 0.1 rad [2]. Family events are classified into two groups: γ families and hadron families. The former consists of only γ rays and the latter of both γ rays and hadrons. The study of these family phenomena is the major subject of emulsion chamber experiments.

All the groups found that there are about 10% of the γ families in which γ rays distribute in a clear multiple cluster pattern. The most probable case is double-core structure, which counts to about 7% of total γ families.

An algorithm of clustering was introduced to describe the cluster behavior of γ-family events [1,13]. Let $E_i, \vec{r}_i$ be the energy, position of the ith photon, R_{ij} the distance between the ith and jth photons, and N the number of photons in a family. All those notations with a subscript c instead of i or j are for the corresponding quantities of a cluster. One calculates $\chi_{ij}=\sqrt{E_i E_j} R_{ij}$ between the two photons. If $\chi_{\min} \equiv \min\{\chi_{ij}, (i,j=1,2,\ldots,N)\}$ is less than a given cutoff value χ_0, e.g., 40 TeV cm [2], the ith and jth particles are then combined into one cluster. The cluster is assigned to a new energy E_i+E_j and a new position at the energy-weighted center of those two particles $(E_i\vec{r}_i+E_j\vec{r}_j)/(E_i+E_j)$. The procedure is repeated until $\chi_{\min} \geqslant \chi_0$ or all members in the family are combined into a single cluster, i.e., $N_c=1$. After clustering, the following additional criteria are applied: (1) For each cluster, $E_c \geqslant 10$ TeV; (2) the total energy of clusters should be more than 80% of the total energy of the family, i.e., $\Sigma E_c \geqslant 0.8 \Sigma E_\gamma$; and (3) $\min\{R_{lk}, (l,k=1,2,\ldots, N_c, l\neq k)\} \geqslant 5 \max\{\langle r_c\rangle_k, (k=1,2,\ldots,N_c)\}$, in which $\langle r_c\rangle_k$ is the average lateral spread of the kth cluster weighted by the energy of its members, i.e., $\Sigma_{i\ni c} |\vec{r}_i - \vec{r}_c| E_i / \Sigma E_i$.

Only the Chacaltaya and Kanbala Collaborations have made their systematic reports on double-core events. Kanbala Collaboration reported four double-core events in Ref. [2]. The group reported two additional events in Ref. [14]. Among these six events, there are five satisfying our criteria. These double-core events were all found among the γ-family data set obtained by the Kanbala experiment in exposures during the years 1980–1986 with a total collecting power of 420 m^2 yr. The total number of γ-family events with $\Sigma E_\gamma \geqslant 200$ TeV accumulated during this period is on the order of 80. The Chacaltaya Collaboration reported 21 double-core events obtained from exposures of 400 m^2 yr in Ref. [1]. Among these 21 events, there are 12 γ-family events with $\Sigma E_\gamma \geqslant 100$ TeV (seven events are hadron families and two events have $\Sigma E_\gamma < 100$ TeV). The total number of γ-family events was not reported by the Chacaltaya group in their paper. Based on the collecting power of the experiment, we estimate that the total γ-family events with $\Sigma E_\gamma \geqslant 100$ TeV is on the order of 200. We found that the frequency of the double-core events is consistent between these two experiments ($\sim 7\%$).

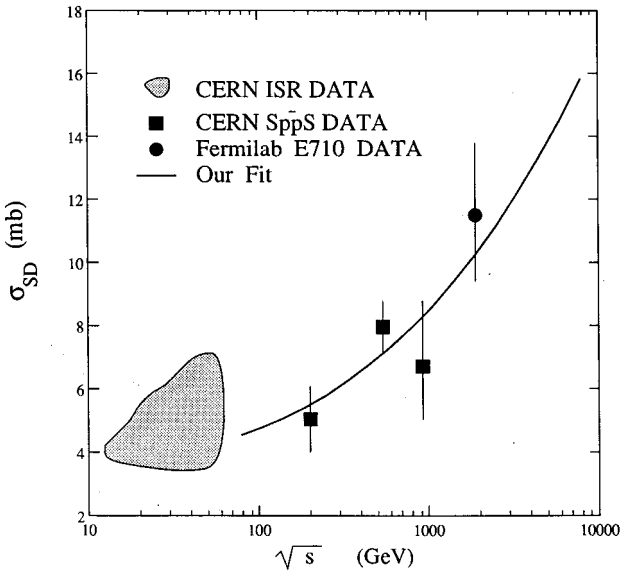

FIG. 1. The cross section for single diffractive (SD) dissociation in pp collision as a function of energy. The ISR data [15] are sketched by the shaded area as low-energy reference points. The curve is the fit to the data from UA4 at $Sp\bar{p}S$ [16] and from E710 at Fermilab Tevatron [17].

IV. INTERACTION MODEL: CONVENTIONAL AND NEW

A. Hadron-hadron interaction model

We divide inelastic hadron-hadron collision into single-diffractive (SD) dissociation and non-single-diffractive (NSD) dissociation two sectors. The cross section for the inelastic interaction at a given lab energy $E_{\rm lab}$ can be expressed as

$$\sigma_{\rm inel}(E_{\rm lab})=\sigma_{\rm SD}(E_{\rm lab})+\sigma_{\rm NSD}(E_{\rm lab}). \tag{4.1}$$

It is experimentally known that $\sigma_{\rm inel}$ increases with energy as $\ln^2 E_{\rm lab}$. It has been found that $\sigma_{\rm SD}(E_{\rm lab})$ also increases with energy as $\ln^2 E_{\rm lab}$, as shown in Fig. 1. Based on cross sections measured at CERN Intersecting Storage Rings (ISR) [15], CERN Super Proton Synchrotron ($Sp\bar{p}S$) [16], and Fermilab Tevatron [17], the high-energy behavior of $\sigma_{\rm SD}(E_{\rm lab})$ can be fitted by

$$\sigma_{\rm SD}(E_{\rm lab})=[a_1+a_2\ln(E_{\rm lab}/1\ {\rm GeV}) + a_3\ln^2(E_{\rm lab}/1\ {\rm GeV})]\sigma_{\rm inel}(E_{\rm lab}), \tag{4.2}$$

with $a_1=0.140$, $a_2=-0.0215$, $a_3=0.00441$, and $\chi^2=1.6/N_{\rm DF}$, shown as the curve in Fig. 1.

For the SD dissociation, we use a Monte Carlo generator developed based on the longitudinal phase space model. This Monte Carlo generator has been demonstrated to be a good description of the SD process at the CERN $Sp\bar{p}S$ energies [18].

The NSD process is described by a hard+soft two-component model [19]. The hard component is characterized by the jet production due to parton-parton scattering. The high-p_T jet production can be precisely calculated with perturbative QCD for hard partonic scatterings. The ''hardness'' condition is given quantitatively in terms of minimum transverse momentum cutoff $p_T^{\rm min}$. In this work, we set $p_T^{\rm min}=4$ GeV c^{-1}. The choice of this cutoff transverse momentum is constrained by the requirement of the unitarity in total inelastic cross section. For those scatterings in which the momentum transfer is lower than this cutoff, perturbative QCD is incorrect and not applicable. For soft interactions, we use a modified version of Chou-Yang model. This version of Chou-Yang model has been demonstrated to be able to reproduce the data of the multihadron production in NSD pp collision at CERN $Sp\bar{p}S$ energies [30,31].

In our QCD calculation of jet production, the evolution of partons before the hard scattering is introduced by the Q^2-dependence of structure function, where Q^2 is the squared momentum transfer in hard scattering between partons, and is taken as $(p_T/2)^2$. We choose the updated version of the parametrization of the distribution function made by Morfin and Tung [20] $f(x,Q^2)$, where x is the fractional momentum carried by a parton. The QCD scale parameter $\Lambda_{\rm QCD}$ is determined by the latest measurement of $\alpha_s(Q^2)$ for $Q^2=m_Z^2$ at CERN e^+e^- collider LEP [21]. The inclusive cross section for jet production is given by

$$\frac{d^2\sigma}{dp_T d\eta}(pp\rightarrow{\rm jet}+X)=\pi p_T e^{\eta}\sum_{a,b}\int dx_1 dx_2 f_a(x_1,Q^2) \times f_b(x_2,Q^2)\hat{s}\frac{d\hat{\sigma}}{d\hat{t}}(ab\rightarrow cd) \tag{4.3}$$

in which the summation runs over all possible parton scattering subprocesses. The subscattering cross section is given as

$$\hat{s}\frac{d\hat{\sigma}}{d\hat{t}}(ab\rightarrow cd)=\frac{\pi\alpha_s^2(Q^2)}{\hat{s}}|\mu(ab\rightarrow cd)|^2\delta(\hat{s}+\hat{t}+\hat{u}). \tag{4.4}$$

The squared invariant amplitude of $2\rightarrow 2$ scattering between partons $|\mu(ab\rightarrow cd)|^2$, can be found for the tree-level cases in Ref. [22].

The calculated inclusive jet cross sections as a function of p_T in different pseudorapidity intervals are compared with data from UA2 [23] in Fig. 2. The agreement between our calculations and the data is quite impressive. It should be noted that our calculation includes only the leading order PQCD.

The total inclusive cross section for *two-jet* production is obtained by integrating Eq. (4.3) over all the kinematically allowed phase space. The exclusive cross section $\sigma_{pp}^{\rm jet}(p_T>4$ GeV $c^{-1})$ is simply the half of the total two-jet cross section because only two jets are produced above the p_T threshold in the entire energy region to which the emulsion chamber experiments are sensitive. Our calculated cross section is plotted in Fig. 3, together with the data from UA1 [24]. The difference between the calculation and the UA1 data reflects the fact that UA1 data were obtained with a lower p_T cutoff [19]. In the same figure, we also present the total inelastic pp cross section $\sigma_{pp}^{\rm inel}$. We plot the data from ISR, $Sp\bar{p}S$, and Tevatron as well as the parametrization of the Particle Data Group [25]. The cross section for the *pure soft* pp interaction is obtained as the difference between $\sigma_{pp}^{\rm inel}$ and $\sigma_{pp}^{\rm jet}(p_T>4$ GeV $c^{-1})$ shown as the dashed curve. The cross section for the pure soft cross section obtained in this way increases

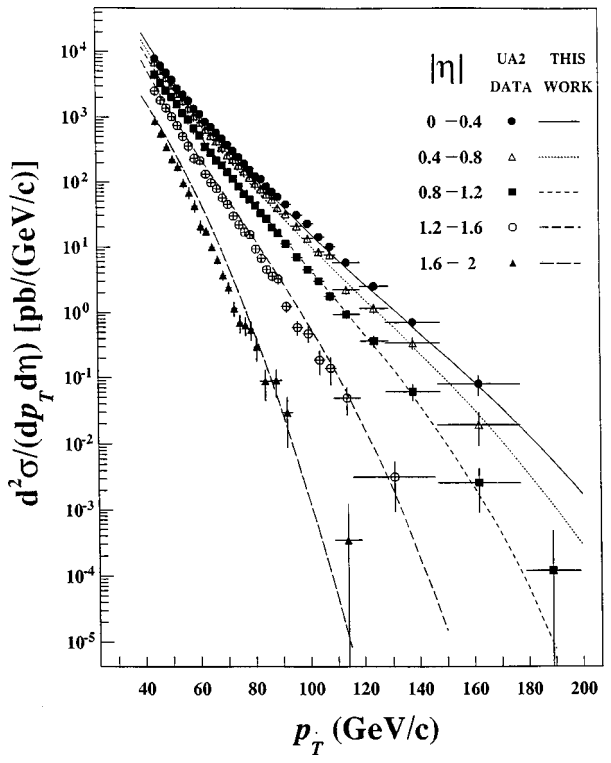

FIG. 2. The inclusive cross section for the jet production in various windows of pseudorapidity η as a function of p_T for $\overline{pp}$ collisions at $\sqrt{s}=630$ GeV. The UA2 data are taken from Ref. [23]. The curves present our perturbative QCD calculations.

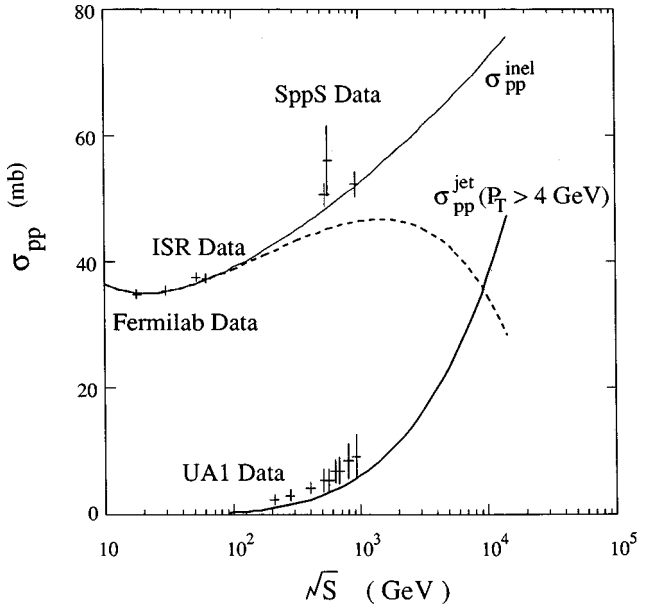

FIG. 3. The energy dependence of various cross sections in pp and $\overline{pp}$ collisions in our two-component model. UA1 [34] measured the jet production cross section with $p_T^{\min}=3$ GeV c^{-1}. Our calculation with $p_T^{\min}=4$ GeV c^{-1} is represented as thick solid line. The cross section for pure soft scattering (dashed line) shows a decrease with $\sqrt{s}$. The data and parametrization of the total cross section for inelastic scattering (thin solid line) are taken from [25].

with energy from $\sqrt{s}=20$ to 1500 GeV and then decreases with energy onward. As the result of the simplified assumption of two-jets, we overestimate the high-p_T jet production at high energies. As we will show later, even though such an overestimated jet production cross section is used in our analysis, the event rates at large p_T still cannot be accounted for by the conventional model of hadron-hadron interactions.

We developed a Monte Carlo algorithm to generate the hadronization of jets based on the independent fragmentation scheme [26]. Since the detector makes no distinction among various hadrons, it is assumed in our generator that only pions are produced in the hadronization process. This allows us to simplify particle yields of various types. There are only two types of jets, jets of quarks and jets of gluons, needed to be considered in the algorithm. In particular, a gluon is treated as a pair of independent quark and antiquark. The splitting function [27]

$$f(x)=\frac{3}{2}[x^2+(1-x)^2] \tag{4.5}$$

controls the distribution of gluon energy, where x represents the fractional energy carried away by the quark.

The fragmentation of quarks is controlled by the fragmentation function with the following parametrization [28]:

$$f(z)=[1+c(Q^2)](1-z)^{c(Q^2)}, \tag{4.6}$$

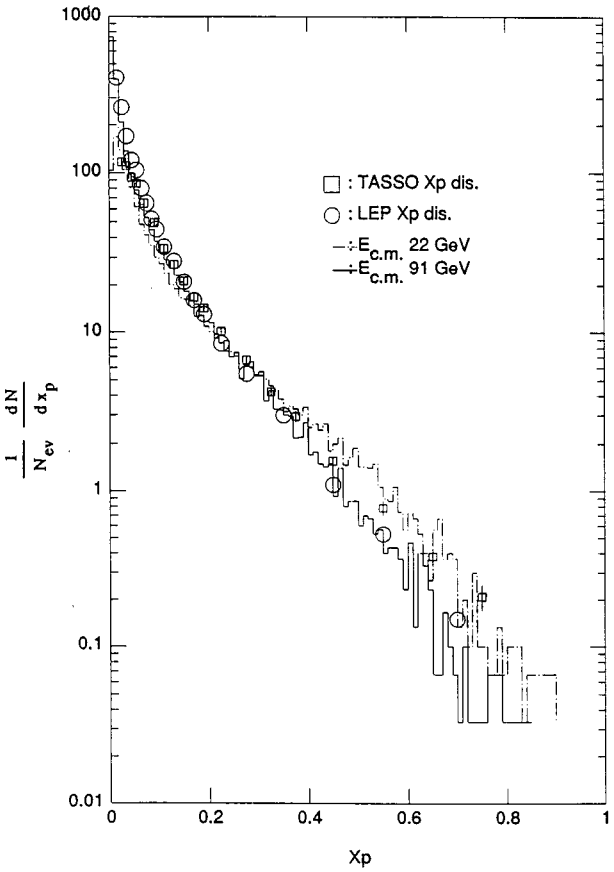

FIG. 4. Fractional momentum distribution of secondaries for hadron production in e^+e^- annihilation. Histograms are our calculations for $\sqrt{s}=22$ GeV (dotted line) and 91 GeV (solid line). Data are taken from [29].

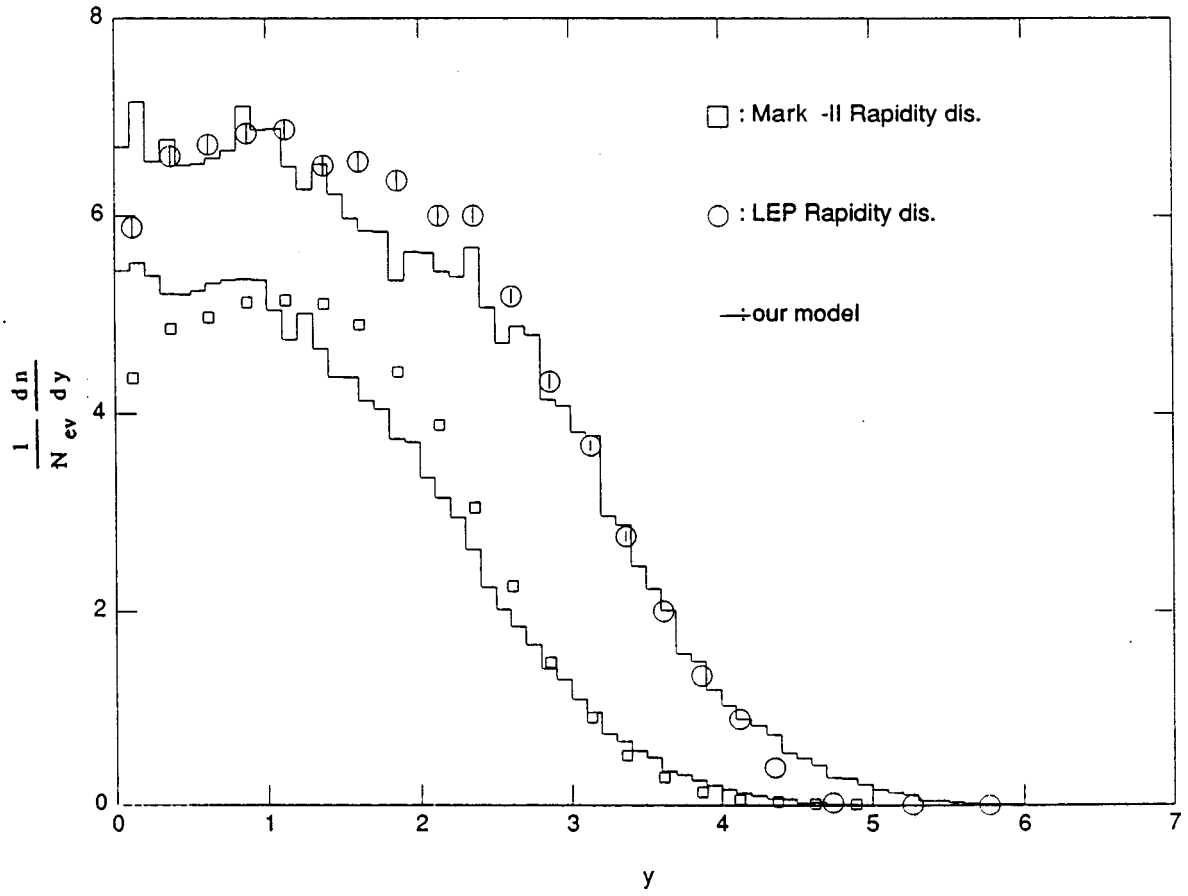

FIG. 5. Rapidity distribution of secondaries for hadron production in e^+e^- annihilation. Histograms are our calculations for $\sqrt{s}=29$ GeV (lower) and 91 GeV (upper). Data are taken from [29].

in which z is the ratio of the light-cone variable $E+p_\parallel$ of the daughter hadron to that of the mother quark. The Q^2 dependence of parameter $c(Q^2)$ reflects the evolution of the quark in the final state. The transverse momentum of produced hadrons is assumed to follow a Gaussian. Its width $\sigma(Q^2,z)$ is a function of Q^2 and z due to the evolution of quarks and the correlation between the longitudinal and transverse momenta of the jet fragmentation. The remaining quarks have the same transverse momentum but in the opposite direction. The fragmentation procedure is repeated for the remaining quarks until its light-cone variable goes below the mass of mesons. To guarantee the conservation of the energy and momentum of the fragmenting system, we adopted an additional procedure [26]. All parameters involved in the jet fragmentation are determined by fitting the hadronic production data in e^+e^- annihilation. Our fragmentation scheme reproduces data from MARK II, TASSO, and LEP [29] reasonably well, as shown in Figs. 4 and 5. The fragmentation of spectators is assumed to follow a soft law.

The geometrical model of Chou and Yang [9] is used to describe the soft interaction. This model assumes that particles produced in a hadronic scattering with a certain impact parameter are stochastically distributed in the phase space. The overall contribution in interactions with various impact parameters gives a single particle inclusive distribution:

$$E\frac{d^3\sigma}{dp^3}=Kg(p_T)e^{-E/T_p}, \tag{4.7}$$

in which T_p is the so-called partition temperature, $g(p_T)$ is the cutoff factor in p_T, and K is an overall normalization factor. A Monte Carlo generator based on this model has been developed by Ding *et al.* [30] and refined by Cao and Ding [31]. It reproduces most of the data at $Sp\overline{p}S$ energies. A set of parameters involved in this model has been carefully extrapolated to higher energies. In the present work, we use this model to generate the *soft* hadronic scattering. The energy dependences of the p_T cutoff factor and partition temperature have been carefully considered.

Let us denote the particle density in phase space element as $(dn/dp_T^2d\eta)_s$, in which the subscript s refers to the contribution to NSD process from different sources. It is obvious that the particle density in NSD process is the statistical average of various components: pure soft (PS), fragmentation of spectators (beam), and fragmentation of jets:

$$\left(\frac{dn}{dp_T^2d\eta}\right)_{\rm NSD}(\sqrt{s})=p_s\left(\frac{dn}{dp_T^2d\eta}\right)_{\rm PS}(\sqrt{s})+p_h\left(\frac{dn}{dp_T^2d\eta}\right)_{\rm beam}(\sqrt{s}-E_{\rm jet})+p_h\left(\frac{dn}{dp_T^2d\eta}\right)_{\rm jet}(\sqrt{s}), \tag{4.8}$$

in which, $p_h=\sigma_{pp}^{\rm jet}(\sqrt{s})/\sigma_{\rm NSD}(\sqrt{s})$ and $p_s=1-p_h$ give the relative probability of jet production and pure soft hadronic scattering, $\sqrt{s}$ is the total energy in the hadron-hadron center-of-mass system, and $E_{\rm jet}$ is the energy carried by the jets. With the approximation of $\sqrt{s}-E_{\rm jet}\sim\sqrt{s}$ for the fragmentation of spectators, the density distribution for pure soft process can be calculated using Eq. (4.8). Namely, we used the measured distribution for NSD and calculated distribution from our Monte Carlo code of PQCD calculation and hadronization of jets to determine the particle density in *pure soft* scattering. The resulting distribution in each energy interval is then fitted by Eq. (4.7). All parameters in the model can be determined in this way. The p_T cutoff factor is determined to be for $p_T<p_T^{\rm min}$

$$g(p_T)=\frac{1}{p_T}e^{\alpha_1 p_T}(B+e^{\alpha_2+\beta p_T^2}), \tag{4.9}$$

in which, parameters α_1, α_2, β, and B depend on the total energy of the interaction. The partition temperature T_p is determined to be a power law of the interaction energy

$$T_p=0.17(\sqrt{s})^{0.701}. \tag{4.10}$$

It should be noted that the above treatment of the soft interaction may, to some extent, oversimplify the case. However, we want to emphasize that the focus of the present study is on high-p_T jet production; the simplified model does not affect our conclusions. This hard+soft two-component model reproduces all the data for NSD pp collision measured at accelerator energies. In Fig. 6, we compare the calculated Feynman variable (x) distribution with data taken at CERN ISR energies [32]. Figure 7 shows a comparison of the calculated pseudorapidity (η) distributions of charged secondaries with data from UA5 and UA7 [33]. Figure 8 is the calculated p_T distribution in comparison with data from UA1 and CDF [34]. It is conceivable that over such a wide energy range from 53 GeV to 1.8 TeV, our model agrees with a variety of data quite well.

This model serves as conventional building blocks in our analysis of γ families. Most of statistical behaviors of γ families can be reproduced using this model in the Monte Carlo simulation of γ families.

B. Hadron-nucleus interaction model

In the atmosphere the cosmic-ray particle interaction takes place with the target of air nuclei. Therefore, we need to develop hadron-nucleus interaction model. Applying the independent nucleon hypothesis, we extend the hadron-hadron interaction model to a hadron-nucleus interaction by including nuclear target effects. This phenomenological approach has been proved to be successful. Among the various nuclear effects, the abnormal nuclear enchancement (ANE) effect is the most important one. The ANE effect has been studied by several experiments [12]. Measurements have been made for ANE at both the jet final state level and single hadron final state level. The data for these two cases are summarized in Figs. 9 and 10, respectively. The ANE exponent index α_F shown as the vertical axis in these figures is defined by

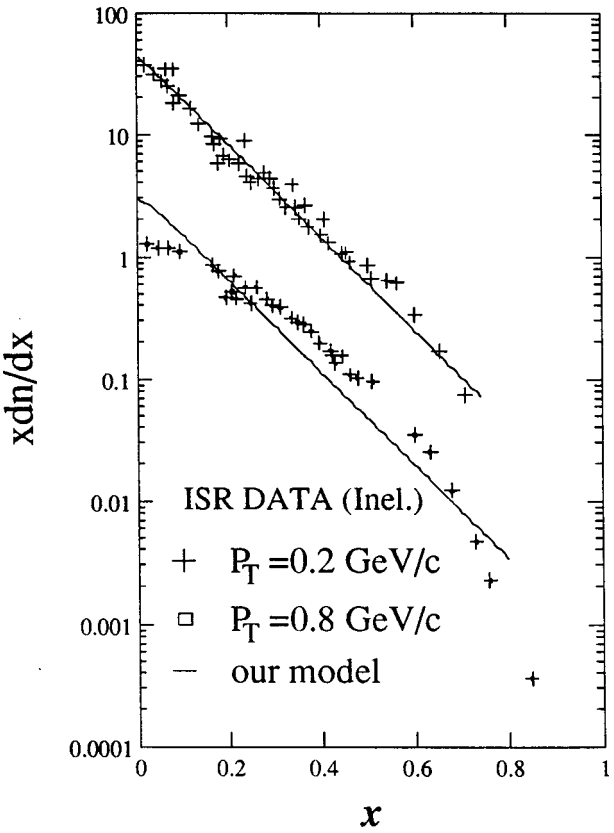

FIG. 6. Distribution of Feynman variable of secondary hadrons in pp collisions. The data are reported in different p_T regions for total inelastic scattering at CERN ISR [32]. Our calculation is carried out only with the NSD scattering.

$$E\frac{d^3\sigma}{dp^3}(pA\to F+X)=A^{\alpha_F(p_T)}E\frac{d^3\sigma}{dp^3}(pp\to F+X), \tag{4.11}$$

where the final state F refers to either jet or single hadron (ptl). The inclusive cross section for pp collision in Eq. (4.11) is given by Eq. (4.3) for jet production and by Eq. (4.7) for single particle production. The obtained ANE parameters from experimental data as a function of p_T (in units of GeV c^{-1}), $\alpha_F(p_T)$, can be expressed as

$$\alpha_{\rm jet}(p_T)=0.667+0.0417\times\frac{(1+0.333p_T)^2}{1+0.000653p_T^{2.5}}$$
$$(\text{for } p_T>4\ \text{GzeV}\ c^{-1}),$$
$$\alpha_{ptl}(p_T)=0.766+0.175p_T-0.0203p_T^2$$
$$(\text{for } p_T\leqslant 4\ \text{GeV}\ c^{-1}). \tag{4.12}$$

These fittings are shown as solid lines in Figs. 9 and 10.

To extrapolate Eq. (4.12) to the ultrahigh energy region for the cosmic-ray air shower simulation, we made the following two additional assumptions. (1) $\alpha_F(p_T)$ is independent of energy. This assumption is valid in the narrow energy range that has been experimentally studied from 70 to 400 GeV, but is no longer valid when energy reaches 800 GeV [35]. Since the new data at 800 GeV has, in fact, shown a weaker effect in comparison with that at 400 GeV, the assumption overestimates the ANE effect at higher energies.

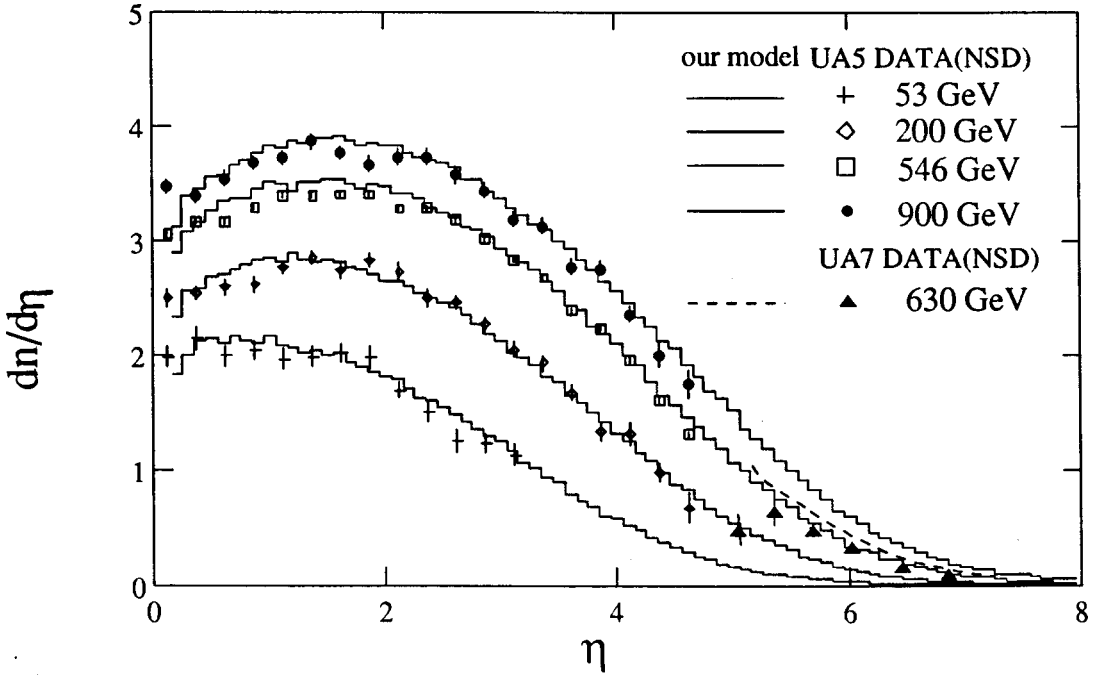

FIG. 7. The pseudorapidity distribution of secondary hadrons in $\overline{pp}$ collisions at CERN $Sp\overline{p}S$. The experimental data [33] are from UA5 at small η and from UA7 at large η (triangles). The solid lines are our calculations for different energies and the dashed line is our calculation for $\eta>5$ at $\sqrt{s}=630$ GeV.

(2) The function forms of $\alpha_{\rm jet}$ and α_{ptl} in the fragmentation region which cannot be measured in collider experiments are the same as those measured in the central region.

Multijet production is another nuclear target effect in our extension from pp interaction model to pA interaction model. Integrating Eq. (4.11) over the phase space for $F=$jet, with mean nucleon number $A=14.5$, the inclusive cross section for jet production in pp scattering $\sigma^{\rm incl}(p+A\rightarrow{\rm jet}+X)$ could be greater than the total inelastic cross section in pA scattering determined by other cosmic-ray experiments as [36]

$$\sigma_{\rm inel}^{p\text{-air}}=290\ {\rm mb}\left(\frac{E_{\rm lab}}{1\ {\rm TeV}}\right)^{k}. \tag{4.13}$$

In Eq. (4.13), $E_{\rm lab}$ is the energy of incident proton in laboratory frame. The exponent k is in the range of $0.04-0.06$ and a value of 0.055 is taken in this paper. According to the geometric scaling law and the consideration of a possibility of multiscattering of the incident proton off the nucleons in target nucleus, the hard component of pA interaction is treated as a multijet production. The average multiplicity of jets is determined as

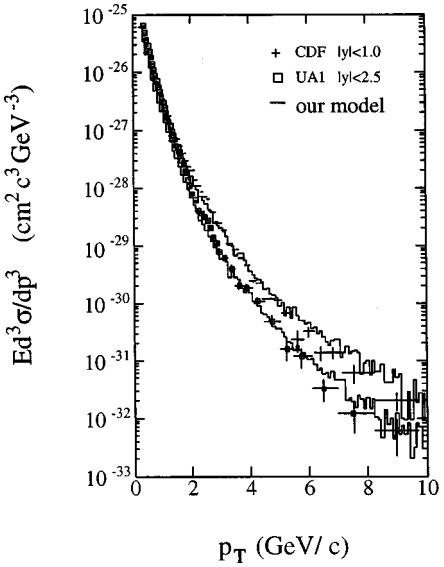

FIG. 8. Transverse momentum spectra of secondaries in $\overline{pp}$ collisions at the different rapidity windows from CDF and UA1 [34] in comparison with our calculations. Note that our model reproduces the data well in the high-p_T region.

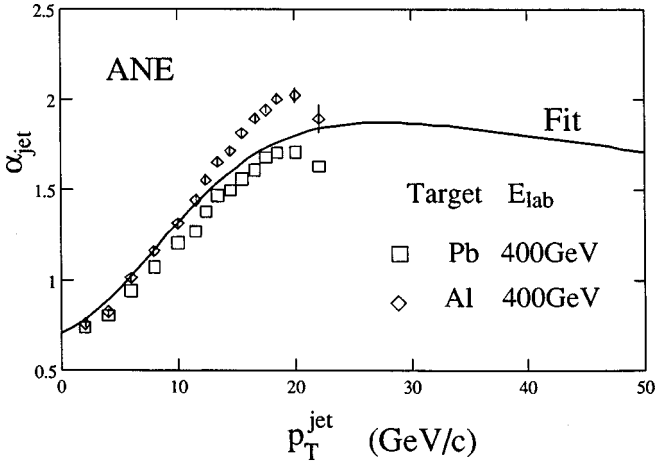

FIG. 9. ANE index $\alpha_{\rm jet}$ of the jet final state in the pA interaction. Data are for 400 GeV proton scattering on lead and aluminum targets. Our extrapolation function gives a behavior of $\alpha_{\rm jet}$ at higher p_T but there is no effect on the pp scattering in the fragmentation region.

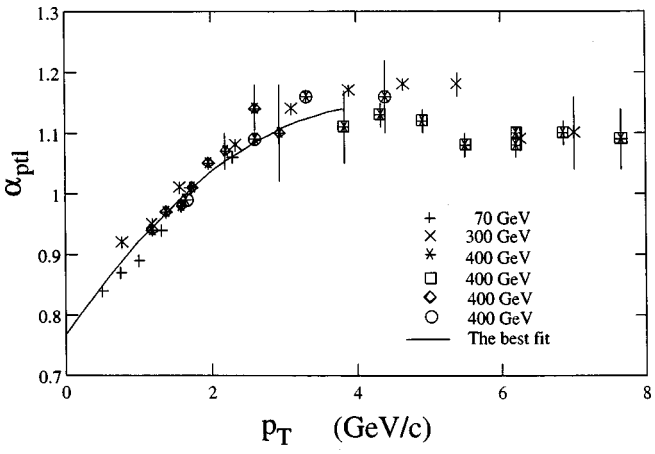

FIG. 10. ANE index α_{ptl} of the single hadron final state in pA interaction. Data [12] from different experiments, target materials and interaction energies are plotted. They show a clear independence of energy from 70 to 400 GeV, especially in the region $p_T<4$ GeV c^{-1}.

$$\langle n_{\rm jet}\rangle=\frac{\sigma^{\rm incl}(p+A\rightarrow{\rm jet}+X)}{\sigma_{\rm inel}^{p\text{-air}}}, \tag{4.14}$$

and the distribution of number of jets is assumed to be uniform.

Another nuclear target effect considered in our model is that the inelasticity of hadron-nucleus scattering is 10–20 % greater than that of hadron-hadron scattering [37]. We neglect other nuclear effects such as the nuclear shadowing on the parton distribution function at small x [38] and possible jet quenching resulting from final state interaction [39]. Because a relative large p_T cutoff, 4 GeV c^{-1}, is taken in our PQCD calculation, hard scattering between partons with small x would mainly contribute to the jet production in the center region. Therefore, the shadowing effect is negligible in our analysis. The interaction of final state of the hard scattering is also not important in our analysis because the target nucleus in the atmosphere is not heavy and the original energy of out going parton is sufficiently high (at least 4 GeV).

C. Quark substructure model

When one seeks a mechanism to explain the high event rates at unreachable high transverse momenta by the ordinary interaction model, it is natural to guess that the interaction probably takes place at a more fundamental level. From the point of view of current QCD parton model, it would be the substructure of quarks. To introduce the mechanism into our Monte Carlo simulation, we use a model of the compositeness of quarks developed by Eichten *et al.* [40]. It is assumed that quarks and leptons are composed of preons. The interaction between the preons is described by a metacolor gauge field. This non-Abelian field is similar to the color force between quarks and is asymptotically free and infrared confining. The inverse of the size of composited constituents provide a characteristic energy scale Λ_c as a parameter of the model. If the interaction energy $\sqrt{\hat{s}}$ were much smaller than Λ_c, the quark would interact each other as a whole particle, otherwise, when $\sqrt{\hat{s}}\geqslant\Lambda_c$, the compositeness of quarks would manifest itself in the interaction, subsequently, an enhancement of the high-p_T particle production would be expected. Eichten *et al.* [40] have pointed out that the compositeness of quarks could be searched for in the study of jet production as an excess in the p_T spectrum of jets with respect to the prediction of QCD.

Without knowing any detail of the interaction between preons, an effective Lagrangian of four-fermion direct contact interaction term (CT) can be written as

$$\mathbf{L}_{qq}=\frac{g^2}{2\Lambda_c^2}\eta_0\overline{q_L}\gamma^\mu q_L\overline{q_L}\gamma_\mu q_L, \tag{4.15}$$

in which g is the coupling constant of a metacolor field and is usually taken as $g^2/4\pi=1$ by choosing an appropriate parameter Λ_c; η_0 is a phase factor which could be $|\eta_0|=1$ as its maximum and is taken as -1 for the constructive interference case in our calculation.

The contribution to the differential cross section for jet production due to Eq. (4.15) is an additional term to the squared amplitude of quark scattering:

$$|\mu(ab\rightarrow cd)|^2=f_{\rm QCD}(\hat{s},\hat{t},\hat{u};\alpha_s)+f_{\rm CT}(\hat{s},\hat{t},\hat{u};\alpha_s,\Lambda_c). \tag{4.16}$$

The explicit formulas of $|\mu(ab\rightarrow cd)|^2$ can be found in Refs. [40] and [41]. The inclusive cross section for jet production is calculated using Eqs. (4.3) and (4.4). The appearance of $f_{\rm CT}$ enhances the cross section for jet production at high p_T. As $\Lambda_c\rightarrow\infty$, $f_{\rm CT}$ vanishes and the calculation returns to pure PQCD [40].

Several experimental groups have searched for the signal of the substructure of quarks at the highest-energy colliders. All of them obtained null results, and the lower limits on Λ_c have been placed. For example, UA2 group [23] reported $\Lambda_c>825$ GeV obtained in the $p\overline{p}$ collision at CERN $Sp\overline{p}S$; and CDF group [42] at Fermilab Tevatron has reported $\Lambda_c>1.4$ TeV at $\sqrt{s}=1.8$ TeV, the most stringent limit obtained so far. We note that the latest result reported by CDF indicates a possible value of $\Lambda_c\simeq1.6$ TeV [43].

It is obvious that the inclusion of the quark substructure in our hadronic interaction model leads to the enhancement of the high-p_T particle production. The degree of the enhancement depends sensitively on the value of Λ_c assumed. For γ families, the case becomes complicated and less obvious because of the biased recording due to the high-energy threshold of the detector. It is critical for us to ask whether the effect of quark substructure affects significantly the behavior of particle production in the fragmentation region. A Monte Carlo calculation has been carried out to prove that there really is a detectable effect in the fragmentation region, e.g., $|\eta|>4$, due to the compositeness of quarks, as shown in Ref. [44].

V. MONTE CARLO SIMULATION OF ATMOSPHERIC INTERACTION AND PROPAGATION

When an ultrahigh-energy cosmic-ray particle, e.g., a proton, enters the atmosphere, it collides with a nucleus in the atmosphere and produces secondary particles. About 1/3 of

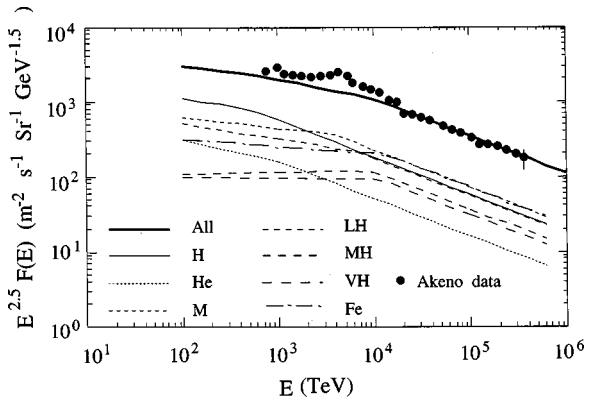

FIG. 11. Differential energy spectra of cosmic rays. The thin lines of different styles correspond to different components. The summation of them (thick solid line) fits the EAS data [47].

the secondaries would be π^0, which immediately decay into photons and the photons subsequently induce electromagnetic cascades in the atmosphere. The charged secondary $\pi^{\pm}$ would either interact with an air nucleus or decay into muons during its flight. The leading particles that carry a significant fraction of incident energy ($1-$ inelasticity) and some secondary particles will induce successive interactions. When the γ rays and hadrons reach the observational level, only those whose visible energies are higher than the detector threshold (~ 4 TeV) would be recorded.

A. Monte Carlo simulation code

A full Monte Carlo code is developed to simulate the propagation process. The interaction models described above are applied to multiparticle production in the propagation. The electromagnetic cascade induced by each photon produced in the decay of $\pi_0's$ is also simulated with a full Monte Carlo code. Our codes are designed to track every particle in those two kinds of cascades until it reaches the observational level or its energy becomes less than the threshold of the detector. The type, energy, position, and direction of all the registered particles are stored. Because the detector only distinguishes electromagnetic component against hadrons, it is blind in detailed particle identification. This simplifies the simulation to a great degree. For example, we assume that leading particles are protons and all charged secondaries are pions. Once a charged pion decays, it is no longer tracked. The vertices (including the strong interaction, decay, e^+e^- pair production of the photon, and the bremsstrahlung of electron) are determined with corresponding free path distribution of pA, πA, lifetime, electromagnetic interaction, and the local density of atmosphere. The U.S. Standard Atmosphere Model is adopted to estimate the density.

B. Primary cosmic-ray composition and spectra

The energy spectra and chemical composition of primary cosmic rays are important input in the study of γ family at ultrahigh energies. The direct measurement of the spectra and composition made possible by balloon-borne experiments such as JACEE reaches only a few times 10^{14} eV/particle [45]. Above this energy, the cosmic ray composition was indirectly obtained by using various techniques such as underground muon detectors [46], extensive air shower arrays [47], and the Fly's Eye observatory [48]. These results are, to a large extent, subject to the correctness of the interaction model used and the adequateness of the method applied, even though the all-particle spectrum has been robustly determined by these techniques. It is well known that there exists a sudden steepening (''knee'') of the spectrum with an exponent index from -2.67 changing into -3.00, around 3500 TeV. So far, the composition around the ''knee'' with our concern ($10^{15}-10^{17}$ eV) remains largely unknown. Hence, we have to extrapolate the direct measurements to higher energies. A conventional procedure of the extrapolation would be guided by the rigidity cutoff model. All the data at the *very high* energy mentioned above, are fitted with a function form $AE^{-\nu}$ for each of the seven groups of cosmic rays, i.e., the proton, helium, medium, lightly heavy, medium heavy, very heavy nuclei, and iron groups. The corresponding mean charge number C, coefficient A, and spectrum index ν are listed in Table I. All the spectra are extended to higher energy over the ''knee'' region with a sharp bending at CE_b according to the rigidity cutoff model and the differential spectrum index is constantly 3.0 for all the seven groups after the bending. The energy E_b at which the spectrum of proton is bent is determined to be 537 TeV. The absolute intensities of the seven groups and the fitting of the data are shown in Fig. 11. The percentage $R(>E)$ of each individual group in the all-particle flux above 10^3 and 10^5 TeV are also listed in the Table I.

C. Detection of shower particles

A simple procedure is developed to simulate the response of the emulsion chamber. The geometric center of an air

TABLE I. The composition and energy spectrum parameters of cosmic rays. The differential spectrum takes the form $AE^{-\nu}$ below the bending energy CE_b. Above the bending energy, all components have $\nu=3.0$. $R(>10^3$ TeV) and $R(>10^5$ TeV) are the relative abundance of each individual component above 10^3 and 10^5 TeV, respectively.

	p	He	M	LH	MH	VH	Fe
C	1	2	7	12	17	23	26
A	1.10	0.871	0.309	0.507	0.0076	0.0125	0.105
ν	2.70	2.79	2.64	2.70	2.47	2.52	2.60
$R(>10^3$ TeV)	23.6	7.1	24.4	17.1	7.1	5.7	15.0
$R(>10^5$ TeV)	13.4	4.0	20.3	16.6	11.4	10.1	24.3

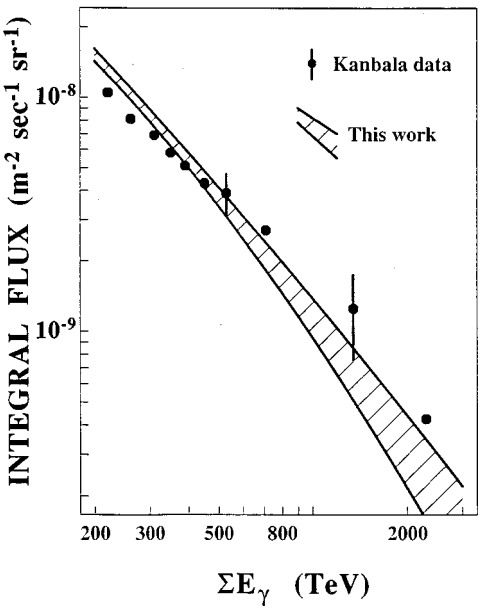

FIG. 12. Flux of the γ-family events versus total energy of the γ family at Kanbala altitude. The uncertainty of our calculation is attributed to the statistical fluctuation and difference in model assumptions.

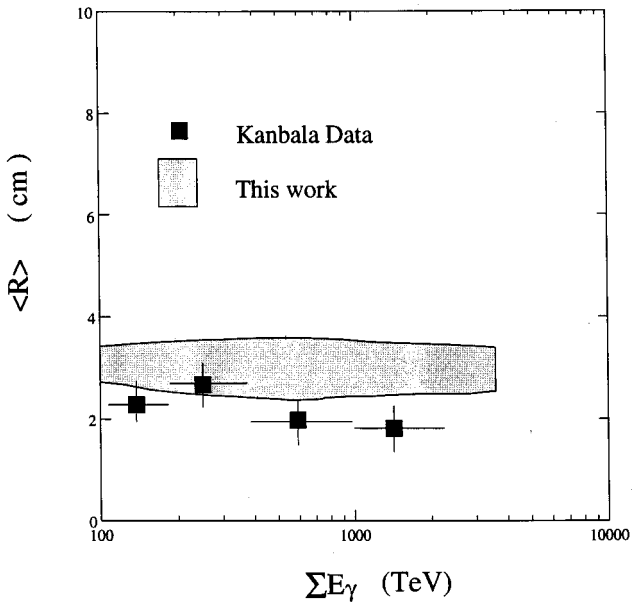

FIG. 13. Average lateral spread of the γ family $\langle R \rangle$ for all events versus total energy of the γ family at Kanbala altitude. The uncertainty of our calculation is attributed to the statistical fluctuation and uncertainties in our model assumptions.

shower is randomly sampled over the area covered by the emulsion chamber. Only those events with the number of photons greater than 4 are considered as observable families. All photons and electrons in a family are assumed to be detectable with 100% efficiency. For a hadron in the family, the vertex of the first interaction in the chamber is sampled according to the interaction cross section of proton or pion with the absorber of the chamber (usually Pb). If the first vertex is too deep, e.g., the distance to the bottom of the chamber is less than 4 radiation lengths, the hadron is undetected because there is not enough material for the shower to develop. If the first vertex is too shallow, e.g., less than 6 radiation lengths, the hadron is misidentified as a photon. The experimentally determined ''visible'' energy for such a photon is that carried by the neutral component of the shower. Our Monte Carlo shows that the visible energy is about 40% of the inelastic interaction energy which is determined stochastically by the inelasticity of hadron-lead interaction. The energy of all ''photons'' in a γ family are summed as the total energy of the family. We only count events with $\Sigma E_\gamma > 200$ TeV for the Kanbala experiment and $\Sigma E_\gamma > 100$ TeV for the Chacaltaya experiment.

VI. SIMULATION RESULTS AND COMPARISON WITH DATA

We obtained about a million air shower samples at Mt. Kanbala and Mt. Chacaltaya levels. A small fraction of the samples obtained with the mixed primary cosmic ray composition was used to study the general properties of family events. The Monte Carlo samples are compared with all the available data about general characteristics of γ families in detail. This provides a basic reference point for the interaction model. Since nearly all double-core events are found to be induced by protons [2], we performed our Monte Carlo simulation for double-core events with only the samples initialized by protons. Imposing the final selection criteria, we have about ~ 6500 γ-family samples with $\Sigma E_\gamma > 200$ TeV at Chacaltaya and ~ 9000 γ-family samples with $\Sigma E_\gamma > 100$ TeV at Kanbala. Three sets of simulations have been carried out assuming (1) the basic model with QCD jet production, (2) the hadron-nucleus interaction with the inclusion of nuclear target effects, and (3) the model with the inclusion of quark compositeness. A comparison of them with the data is presented as follows.

A. General properties of γ-family events

The intensity of γ-family events is an important observable in emulsion chamber experiment. It is believed that the absolute intensity would depend on the total inelastic scattering cross section of a cosmic-ray particle with atmospheric nuclei, the inelasticity of the interaction, and the composition of cosmic rays. Given the composition of cosmic rays and their interaction cross sections with atmospheric nuclei determined by other experiments, we obtained the energy spectrum of the family events via Monte Carlo simulations. The calculated family intensity is consistent with the data observed by the Kanbala experiment [2] as shown in Fig. 12. This agreement confirms that our two component interaction model, including the enhanced jet production and the nuclear effects, gives a correct overall description of the ultrahigh-energy interaction in the forward region. Although the Chou-Yang model has a well-known feature of breaking down the Feynman scaling, the model of the SD and NSD processes implemented by careful consideration of enhanced inelasticity for pA collisions describes correctly the attenuation property of the ultrahigh-energy air shower in its propagation.

The lateral spread of γ families is another important observable in the Kanbala experiment [2]. Two variables $\langle R \rangle$ and $\langle ER \rangle$ are introduced as a measure of the average transverse momentum for all secondaries in hadron-nucleus inter-

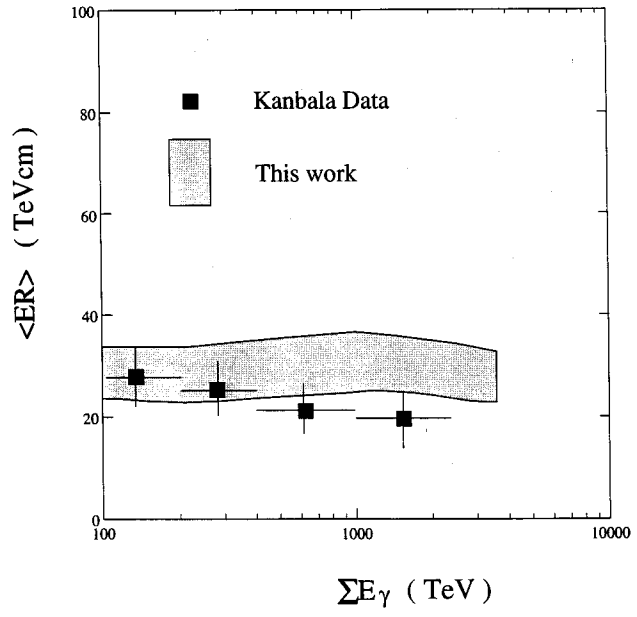

FIG. 14. Average lateral spread of the γ family $\langle ER \rangle$ for all events versus total energy of the γ family at Kanbala altitude. The uncertainty of our calculation is attributed to the statistical fluctuation and difference in model assumptions.

actions. They are of particular relevance to the study of double-core events. The measurements of $\langle R \rangle$ and $\langle ER \rangle$ versus ΣE_γ serve as a constraint to possible overall enhancement of high-p_T particle production in the model. These two observables are calculated and are shown in Figs. 13 and 14 as a function of the total energy of the γ family. The uncertainties, represented as the shadow areas in these figures, are due to differences between model assumptions together with statistical fluctuation. It is seen that our simulation agrees with the data reasonably well except for a slight overestimate for high-energy families. It is also found that $\langle ER \rangle$ agrees with the data better than $\langle R \rangle$. This might be attributed to an experimental bias by which some possible members of a family are simply missed in the scanning just because they locate too far away from the center of the family [2].

Particles in Monte Carlo family samples show the tendency of multicluster structures. This feature becomes more significant after applying the procedure of clustering as described in Sec. III. The distribution of the number of clusters in a family is compared to the data reported by the Kanbala group [2]. They agree with each other. As shown in Fig. 15, the distribution is not very sensitive to the changes in the interaction model. It is found that about 12% of the γ families have cluster structures, a frequency that is remarkably in agreement with the data.

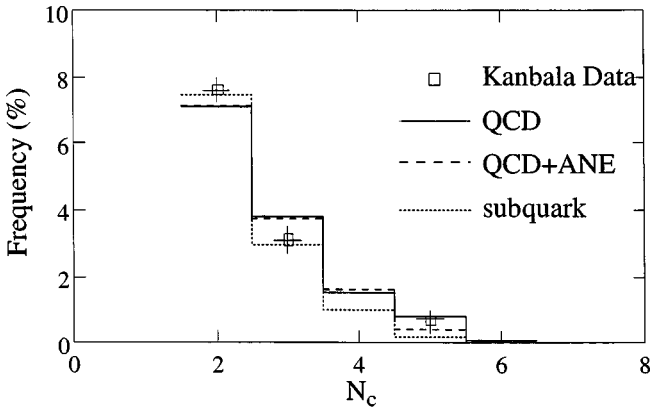

FIG. 15. Distribution of average number of clusters in a γ family for all the Kanbala data.

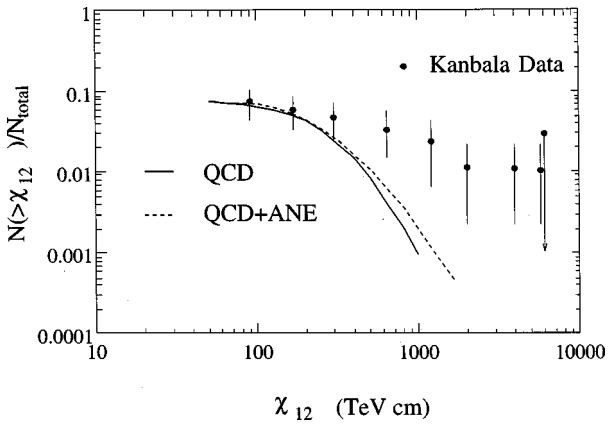

FIG. 16. Distribution of χ_{12} of double-core events in Kanbala experiment. Corresponding simulation results based on the basic model (solid curve) and the model with the ANE effect are plotted.

In summary, the overall agreements of our simulation with the general features of the γ families observed in the Kanbala experiment are established. The confidence of our model gained in this comparison put us in a position to pursue further study of the double-core phenomenon.

B. Properties of double-core events

For families with two clusters, the so-called double-core events, there are more observational quantities reported by experimental groups. The compilation of experimental data sets obtained by the Kanbala and Chacaltaya Collaborations is described in Sec. III. The integral frequency spectra of the observable χ_{12} are plotted in Figs. 16 and 17 for Kanbala and Chacaltaya, respectively. The vertical axes of these figures represent the ratio of the number of double-core events with $>\chi_{12}$ to the number of all family events. The solid curves in those two figures show the prediction of our basic model

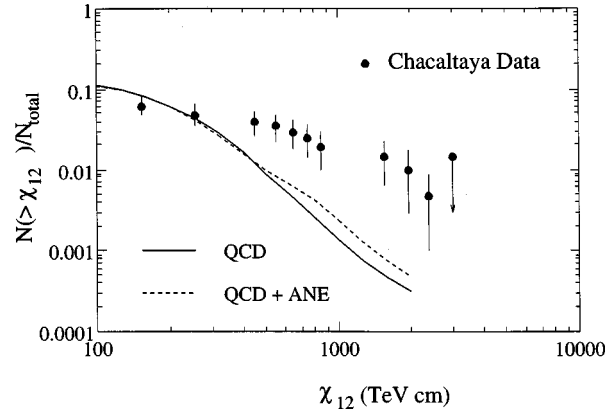

FIG. 17. Distribution of χ_{12} of double-core events in Chacaltaya experiment. Corresponding simulation results based on the basic model (solid curve) and the model with the ANE effect are plotted.

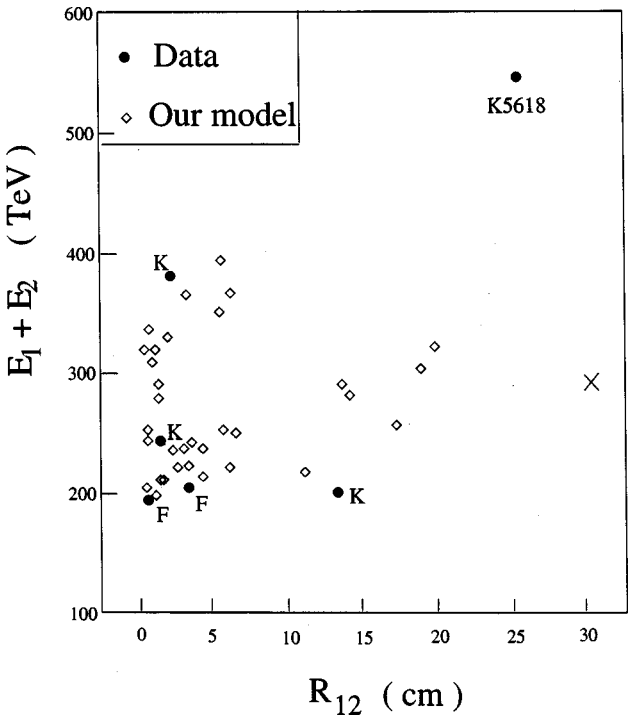

FIG. 18. The correlation between E_1+E_2 and R_{12} for double-core events observed in the Fuji (F) and Kanbala (K) experiments. The simulation is carried out only for Kanbala altitude. K5618 is the event with the greatest χ_{12}. Cross indicate the only Monte Carlo event with a long distant between cores.

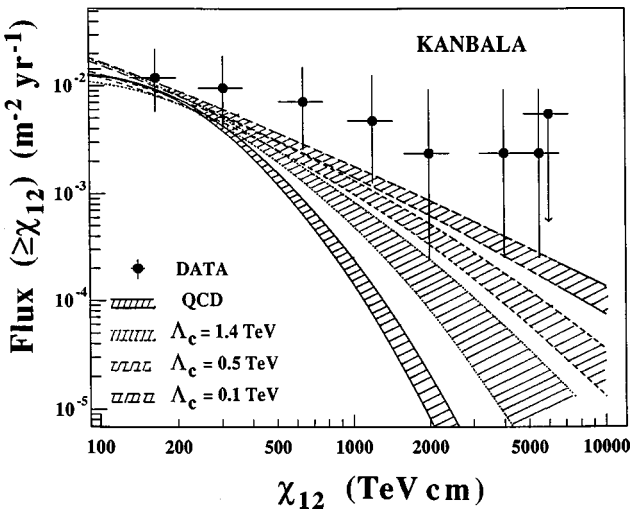

FIG. 19. Integral flux of double-core γ-family events with χ_{12} observed in emulsion chambers installed on the top of Mt. Kanbala, in comparison with our calculations. Data are compiled from Refs. [2,14].

with the PQCD jet production. We find huge excesses of the event rates over the prediction in both sets of data. In the region of $\chi_{12}<300$ TeV cm, the model reasonably reproduces the data. However, at large χ_{12} around 1000 TeV cm, the prediction is almost one order of magnitude lower than the data. In general, the uncertainty of the PQCD calculation is smaller than one order of magnitude. The huge discrepancy between the data and our model prediction has to be caused by some certain physical processes.

We also examined the correlation between the total energy of two clusters and the spatial distance between them. Figure 18 shows the scattering plots for the Kanbala data. Some of our Monte Carlo samples are also plotted for comparison. The population of the scattering points relatively concentrates at the corner with lower energy and shorter distance. Double-core families having $R_{12}>20$ cm are rarely found in our Monte Carlo samples. In the Kanbala data, event K5618 is located far away from the main population. In our Monte Carlo events, even the sample size is a factor of 10 larger than the experimental data, there are only five events with $R_{12}>25$ cm and only one with $R_{12}\sim 30$ cm.

VII. CONCLUSIONS AND DISCUSSIONS

The distribution of χ_{12} and the relation between E_1+E_2 and R_{12} for double-core events from both the Kanbala and Chacaltaya experiments are *inconsistent* with the prediction from the Monte Carlo simulation based on the extrapolation of *conventional* physics. The discrepancies are so large that neither the uncertainties involved in our interaction models, nor the statistical errors of the data are sufficient to account for them. We have to attribute them to the possible onset of certain physical mechanisms which have not been included in our interaction models.

Nuclear target effects are expected to make a considerable contribution to the high event rates at large χ_{12}. The results, plotted as the dashed curves in Figs. 16 and 17, show that nuclear target effects indeed increase the event rates at large χ_{12}. But they are certainly *not* enough to explain the data. It should be pointed out that nuclear target effects are included in our current calculation in such a way that the production of high-p_T particles are already overestimated, as we discussed in Sec. IV.

Recent calculations of next-to-leading order PQCD by Giele *et al.* [11] call for the attention to the significant impact on two-jet differential cross sections where one of the jets has large c.m. rapidity and high p_T. The enhancement of jet cross sections relative to the leading order calculations clearly increases with the increasing rapidity and transverse momentum of the jet. For instance, the enhancement is up to a factor of 2 in the region of $10\leqslant p_T\leqslant 20$ GeV c^{-1} and $\eta\geqslant 4$ to which the cosmic ray experiments are sensitive. Although the effect of this enhancement on the rate of cosmic-ray events could not be accurately evaluated due to the complications of multiple interactions of cosmic-ray interactions and biased detection in emulsion experiments, our estimate indicates that it could not contribute to event rates at $\chi_{12}\sim 1000$ TeV cm by more than one order of magnitude. Therefore, it seems that the existing more than one order of magnitude excess of the data over the model prediction is hardly accounted for by solely including higher order corrections in PQCD calculations. A careful evaluation based on Monte Carlo simulations with next-to-leading order QCD jet production will be performed in the future.

The effect of the compositeness of quarks is introduced using an effective model with a scale Λ_c. The corresponding simulation with a set of choices of Λ_c including $\Lambda_c=1.4$ (the latest upper limit from pp collider experiments) is carried out. The enhancement of the prediction in the χ_{12} distribution is readily seen in Fig. 19 for Kanbala and Fig. 20 for Chacaltaya. The calculation results using a conventional

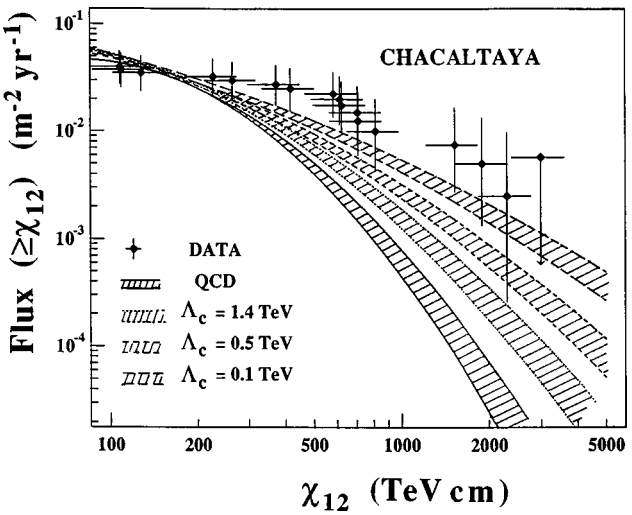

FIG. 20. Integral flux of double-core γ-family events with χ_{12} observed in emulsion chambers installed on the top of Mt. Chacaltaya, in comparison with our calculations. Data are compiled from Ref. [1].

model are also plotted in the same figures for comparison. It is noted that the effect of subquark structure is not enough to be the only reason for the excesses.

The scale of subquark structure is lowered in an attempt to fit the data. In Figs. 19 and 20, the results corresponding to $\Lambda_c = 500$ and 100 GeV are plotted, respectively. The experimental χ_{12} distributions are marginally fitted by the simulation with a very low scale $\Lambda_c = 100$ GeV. We found one event with $R_{12} \sim 30$ cm out of 93 Monte Carlo double-core events at Kanbala level, shown as crosses in Fig. 18.

The χ_{12} distributions predicated by models with the quark compositeness are closer to the data than those produced by models without the quark compositeness. The degree of the deviation decreases with a decreasing characteristic energy scale Λ_c. This indicates that the mechanism of subquark structure could account for the deviation observed in χ_{12} distributions and in the correlation between $E_1 + E_2$ and R_{12}. But it cannot be the only reason because calculations with $\Lambda_c > 1.4$ TeV allowed by the latest collider experiments are not sufficient to explain the data. For the quark substructure to be the only reason for this discrepancy, the date would require an unrealistic Λ_c as low as 100 GeV.

Even though 100 GeV may be an unrealistic energy scale for quark compositeness as indicated by current collider experiments, the study gives us an idea that how large the transverse momentum could be needed in the hadron-nucleus interaction in order to explain the double-core phenomenon. In a more general sense, the inclusion of the quark substructure model is used to estimate quantitatively what kind of mean p_T and p_T distribution the data require as an important feature of the possible new physics. We emphasize that the family events are results of successive particle productions. A value of the quark p_T is sampled in every interaction in the simulated air showers. It is found that a stronger enhancement is expected at $p_T \simeq 10 \sim 20$ GeV c^{-1} in the fragmentation region of hadron-hadron or hadron-nucleus interaction, although it is really a small p_T comparing that in center region. It is proved that there is only 1% enhancement in jet production with $p_T \sim 10$ GeV c^{-1} in the fragmentation region $|\eta| > 4$, due to the effect of subquark at ultrahigh energy [44].

In our present work, the high-p_T jet production in the central region is introduced by using the subquark model with $\Lambda_c = 100$ GeV. The explanation of the double-core phenomenon may involve new mechanism for high-p_T particle production in the forward region. In this regard, new physics in connection with SD process or the fragmentation of spectators with high-p_T valence quarks would be interesting to explore. For example, the study of the so-called hard single dissociation with a J/ψ production might be of potential interest.

Finally, we point out that the energy region in which we observe that discrepancy can be explored in the next generation of colliders such as the Large Hadron Collider (LHC). It seems to be particularly feasible to study the new physics indicated by our analysis with a wide acceptance detector system designed for the dedicated study of forward physics at the LHC [49,50]. In such a detector system, the signal could be readily detectable as a large departure from the standard QCD, as a consequence of either the quark compositeness or other new physics.

ACKNOWLEDGMENTS

This work was supported in part by Chinese Natural Science Foundation (Z.C., L.K.D., and Q.Q.Z.), and by the U.S. Department of Energy under Contract Nos. DE-FG06-91ER40637 (Z.C.) and DE-AC03-76SF00098 (Y.D.H.).

[1] C. M. G. Lattes, Y. Fujimoto, and S. Hasegawa, Phys. Rep. **65**, 151 (1980).
[2] J. R. Ren *et al.*, Phys. Rev. D **38**, 1404 (1988).
[3] Q. Q. Zhu, L. K. Ding, Y. D. He, C. L. Jing, G. R. Jing, G. J. Wang, C. Wei, and M. Zhang, J. Phys. G **16**, 295 (1990).
[4] D. Cline, F. Halzen, and J. Luthe, Phys. Rev. Lett. **31**, 491 (1973).
[5] F. Halzen and D. A. Morris, Phys. Rev. D **42**, 1435 (1990).
[6] Y. D. He, Q. Q. Zhu, and A. X. Huo, Phys. Lett. B **271**, 440 (1991).
[7] Z. Cao, L. K. Ding, Q. Q. Zhu, and Y. D. He, Phys. Rev. Lett. **72**, 1794 (1994).
[8] L. K. Ding, Q. Q. Zhu, C. L. Jing, G. R. Jing, and Y. D. He, Sci. Bull. **33**, 726 (1988).
[9] T. T. Chou and C. N. Yang, Phys. Rev. D **32**, 1692 (1985).
[10] M. Benayoun, Ph. Leruste, J. L. Narrjoux, and R. Petronzio, Report No. CERN-TH 4368/86 (unpublished); G. L. Kasha *et al.*, Phys. Rev. Lett. **36**, 1007 (1976); E609 Collaboration, C. Naudet *et al.*, *ibid.* **56**, 808 (1986); BEBC WA59 Collaboration, P. J. Fitch *et al.*, Z. Phys. C **31**, 51 (1986).
[11] W. T. Giele, E. W. N. Glover, and D. A. Kosower, Phys. Rev. Lett. **10**, 2019 (1994).
[12] J. W. Cronin *et al.*, Phys. Rev. D **11**, 3105 (1977); R. L. McCarthy *et al.*, Phys. Rev. Lett. **40**, 213 (1978); D. A. Finley

et al., *ibid.* **42**, 1031 (1979); D. Antreasyan *et al.*, Phys. Rev. D **19**, 764 (1979); H. J. Frisch *et al. ibid.* **27**, 1001 (1983); V. V. Abramov *et al.*, Pis'ma Zh. Éksp. Teor. Fiz. **38**, 296 (1983) [JETP Lett. **38**, 352 (1983)]; Y. B. Hsiung *et al.*, Phys. Rev. Lett. **55**, 457 (1985).

[13] M. Akashi *et al.*, Nuovo Cimento A **65**, 355 (1982); M. Amenomori *et al.*, in *Proceedings of the 18th International Cosmic Ray Conference*, Bangalore, India, edited by N. Durgaprasad *et al.* (TIFR, Bombay, 1983), Vol. 11, p. 57.

[14] J. R. Ren *et al.*, High Energy Phys. Nucl. Phys. **13**, 97 (1989).

[15] M. G. Albrow *et al.*, Nucl. Phys. **B108**, 1 (1976); D. S. Ayres *et al.*, Phys. Rev. Lett. **37**, 1724 (1976); R. L. Cool *et al.*, *ibid.* **47**, 701 (1981).

[16] UA4 Collaboration, Phys. Lett. B **198**, 583 (1987).

[17] E710 Collaboration, Phys. Lett. B **243**, 158 (1990).

[18] Q. Q. Zhu, L. K. Ding, G. J. Wang, and Y. D. He, J. Phys. G **20**, 1383 (1994).

[19] For a review, see, e.g. F. Halzen, in *Proceedings of 21st International Cosmic Ray Conference*, Adelaide, Australia, 1989, edited by R. Protheroe (Graphic Services, South Australia, 1990), Vol. 12, p. 101.

[20] J. G. Morfin and W. K. Tung, Z. Phys. C **52**, 13 (1991).

[21] S. Bethke, Report No. CERN-PPE/91-36, 1991 (unpublished).

[22] B. L. Combridge *et al.*, Phys. Lett. **70B**, 234 (1977).

[23] UA2 Collaboration, J. Alitti *et al.*, Phys. Lett. B **257**, 232 (1991).

[24] UA1 Collaboration, Nucl. Phys. **B309**, 405 (1988).

[25] Particle Data Group, K. Hikasa *et al.*, Phys. Rev. D **45**, S1 (1992).

[26] A. Ali *et al.*, DESY Internal Report No. T-80/01 (unpublished).

[27] G. Altarili and G. Parisi, Nucl. Phys. **B126**, 298 (1977).

[28] T. Sjötrand, Int. J. Mod. Phys. A **3**, 751 (1988).

[29] Mark II Collaboration, A. Pettersen *et al.*, Phys. Rev. D **37**, 1 (1988); TASSO Collaboration, M. Althoff *et al.*, Z. Phys. C **22**, 307 (1984); TASSO Collaboration, W. Braunschweg *et al.*, *ibid.* **45**, 193 (1989); ALEPH Collaboration, Phys. Lett. B **234**, 209 (1990).

[30] L. K. Ding *et al.*, High Energy Phys. Nucl. Phys. **12**, 731 (1988).

[31] Z. Cao and L. K. Ding, High Energy Phys. Nucl. Phys. **18**, 990 (1994).

[32] G. Giacomelli and M. Jacob, Phys. Rep. **55**, 1 (1979).

[33] UA5 Collaboration, G. J. Alner *et al.*, Phys. Lett. **160B**, 199 (1985); A. Osawa, Prog. Theor. Phys. **84**, 50 (1990).

[34] UA1 Collaboration, Phys. Lett. **118B**, 169 (1982); CDF Collaboration, Phys. Rev. Lett. **61**, 1821 (1988).

[35] P. B. Straub *et al.*, Phys. Rev. Lett. **68**, 452 (1992).

[36] T. Yuda, in *Proceedings of the 22nd International Cosmic Ray Conference*, edited by D. O'Sullivan (Dublin Institute for Advanced Studies, Dublin, 1991), Vol. 5, p. 313.

[37] L. W. Jones, in *Proceedings of the 18th International Cosmic Ray Conference* [13], Vol. 5, p. 17.

[38] European Muon Collaboration, J. Ashman *et al.*, Phys. Lett. B **202**, 603 (1983); European Muon Collaboration, M. Arneodo *et al.*, *ibid.* **211**, 493 (1988); L. L. Frankfurt and M. I. Strikman, Phys. Rep. **160**, 235 (1988); V. Barone *et al.*, Z. Phys. C **58**, 541 (1993).

[39] M. Gyulassy and M. Plümer, Phys. Lett. B **243**, 432 (1990); X. N. Wang and M. Gyulassy, Phys. Rev. Lett. **68**, 1480 (1992).

[40] E. J. Eichten, I. Hinchliffe, K. D. Lane, and C. Quigg, Rev. Mod. Phys. **56**, 579 (1984), and references therein.

[41] E. J. Eichten, K. D. Lane, and M. E. Peskin, Phys. Rev. Lett. **50**, 811 (1983).

[42] CDF Collaboration, F. Abe *et al.*, Phys. Rev. Lett. **68**, 1104 (1992).

[43] CDF Collaboration, F. Abe *et al.*, Phys. Rev. Lett. **77**, 438 (1996).

[44] Z. Cao and Y. D. He, Mod. Phys. Lett. A **10**, 267 (1995).

[45] JACEE Collaboration, T. H. Burnett *et al.*, Astrophys. J. **349**, L25 (1990); JACEE Collaboration, in *Proceedings of the 22nd Cosmic Ray Conference* [36], p. 57.

[46] MACRO Collaboration, M. Aglietta *et al.*, Phys. Lett. B **337**, 376 (1994).

[47] M. Nagano *et al.*, J. Phys. G **10**, 1295 (1992).

[48] T. K. Gaisser *et al.*, Phys. Rev. D **47**, 1919 (1993).

[49] J. D. Bjorken, Int. J. Mod. Phys. A **7**, 4189 (1992).

[50] K. Eggert (private communication).